RSC Advances

PAPER

View Article Online
View Journal | View Issue

Cite this: *RSC Adv.*, 2017, **7**, 25746

Facile synthesis of Au/Al_2O_3 nanocomposites for improving the detection sensitivity of adenosine triphosphate†

Li Xu, Qin Xu, Xiaoyu Guo, Ye Ying, Yiping Wu,* Ying Wen and Haifeng Yang *

Received 30th March 2017
Accepted 26th April 2017

DOI: 10.1039/c7ra03683c

rsc.li/rsc-advances

Alumina is widely recognized as chemically inert, and resistant to oxidation and high temperature. In this study, Au/Al_2O_3 nanocomposites (NCs) were prepared by a facile method and were used as a surface enhanced Raman scattering (SERS) substrate for detection of adenosine triphosphate (ATP). This Au/Al_2O_3-based SERS substrate demonstrated good sensitivity with the lowest detectable concentration of 5×10^{-9} M for ATP and a good linear relationship ranging from 5×10^{-5} to 5×10^{-9} M. The strategy of improvement of SERS detection sensitivity for ATP was based on the consideration of ATP captured by such SERS substrate *via* chelation of aluminum and phosphates, which was validated by X-ray photoelectron spectroscopy. In addition, alumina as a supporting material could be expected to prolong the stability of such a SERS substrate.

1 Introduction

Surface enhanced Raman scattering (SERS) was discovered in the 1970s[1–3] and SERS effects are generally attributed to chemical (CHEM) enhancement[2] and electromagnetic (EM) enhancement.[3] SERS is ultrasensitive and can detect some analytes at single molecular level.[4–6] SERS can also be utilized in multiplex detection due to structural and fingerprint information with excellent frequency resolution.[7,8] Therefore, SERS spectroscopy, as a non-destructive and *in situ* technique, has been widely applied in food safety,[9,10] biomarker detection,[11–13] forensic science,[14,15] environment monitoring[16–18] and other trace level analysis fields.[19,20]

Alumina is well known as being chemically inert and tolerant of oxidation and high temperature. Nanocomposites (NCs) formed with alumina and noble metals have been widely studied. Alumina was used to support ultrafine gold particles to act as Al_2O_3-supported Au catalysts.[21,22] Alumina nanoporous layers have demonstrated great potential as stable SERS platforms. For example, porous anodic aluminum oxide (AAO) with a well-arranged hexagonal order was synthesized as a SERS-active substrate.[23–26] Au/Al_2O_3 NCs and Ag/Al_2O_3 NCs synthesized *via* the sonoelectrochemical method improved the thermal stability of the SERS substrates and exhibited excellent sensitivity.[27–29]

In addition, alumina is widely employed as a polar adsorbent in chromatographic separations and has high affinity for molecules with strong polarity, indicating that alumina has the potential to selectively bind molecules. Based on this principle, Van Duyne *et al.*[30] deposited a sub-1 nm alumina layer on silver film-over-nanosphere (AgFON) substrates and exploited the high adsorption affinity of carboxylic acids to alumina-modified AgFON surfaces to detect calcium dipicolinate, a bacillus spore biomarker. In addition to carboxylic acid, aluminum can adsorb phosphorus compounds, which is critical for soil fertility. Feng *et al.*[31] studied the size-dependent sorption of myo-inositol hexakisphosphate (IHP) and inorganic phosphate (KH_2PO_4, Pi) on nano-γ-Al_2O_3, and they found that surface complexation is the main mechanism for IHP and Pi sorption on large size γ-Al_2O_3 (35 nm and 70 nm), while there also exists a surface precipitation mechanism for very small size γ-Al_2O_3 (5 nm). Chen *et al.*[32] used pigeon ovalbumin, a phosphate protein to functionalize Fe_3O_4@Al_2O_3 magnetic NPs through aluminum phosphate chelation to selectively detect Shiga-like toxin-1B.

Adenosine triphosphate (ATP) acts as a universal energy carrier in biological systems and hydrolyzes to generate energy for muscle contraction and several cytological processes.[33,34] A Raman spectroscopic experiment was conducted to study the interaction of divalent metal ions with the adenine moiety of ATP in 1979.[35] SERS spectra of ATP adsorbed on silver electrodes and the influence of voltage, pH value, and divalent metal ions on the SERS spectra of ATP were further studied in 1989.[36] In recent years, an aptamer biosensor with gold nanostar@Raman label@SiO_2 core–shell nanoparticles was constructed to detect ATP.[37] A 3D SERS structure made of Au/cicada wing was recently

The Education Ministry Key Lab of Resource Chemistry, Shanghai Key Laboratory of Rare Earth Functional Materials, Shanghai Municipal Education Committee, Key Laboratory of Molecular Imaging Probes and Sensors, Department of Chemistry, Shanghai Normal University, Shanghai, 200234, China. E-mail: hfyang@shnu.edu.cn; yipingwu@shnu.edu.cn; Tel: +86-21-64321701

† Electronic supplementary information (ESI) available: SERS spectra of 10^{-4} M ATP with different pH (Fig. S1). XPS patterns of P 2p of ATP adsorbed on Al_2O_3 and pure ATP (Fig. S2). SERS spectra of 10^{-5} M ATP and 10^{-5} M adenosine on Au/Al_2O_3 NCs, respectively (Fig. S3). See DOI: 10.1039/c7ra03683c

developed for the quantitative determination of ATP in a mixture of ATP and ADP (adenosine diphosphate).[38] However, the above approaches to detect ATP are either laborious or require special materials.

In this study, we synthesize Au/Al_2O_3 NCs by a facile chemical pathway for the sensitive SERS detection of ATP. ATP can be adsorbed onto the γ-Al_2O_3 surface to form surface complexation *via* aluminum phosphate chelation. The high adsorption affinity of ATP molecules to Au/Al_2O_3 NCs will further increase SERS detection sensitivity and improve the ultimate detection limit. The acquired lowest detectable concentration is 5×10^{-9} M with a linear range from 5×10^{-5} to 5×10^{-9} M.

2 Experimental

2.1. Materials

Chloroauric acid ($HAuCl_4 \cdot 4H_2O$, 99.9%) and sodium citrate ($Na_3C_6H_5O_7 \cdot 2H_2O$, 99.8%) were obtained from Sinopharm Chemical Reagent Co., Ltd. γ-Al_2O_3 (20 nm) was obtained from Aladdin Industrial Corporation. ATP was purchased from Sigma-

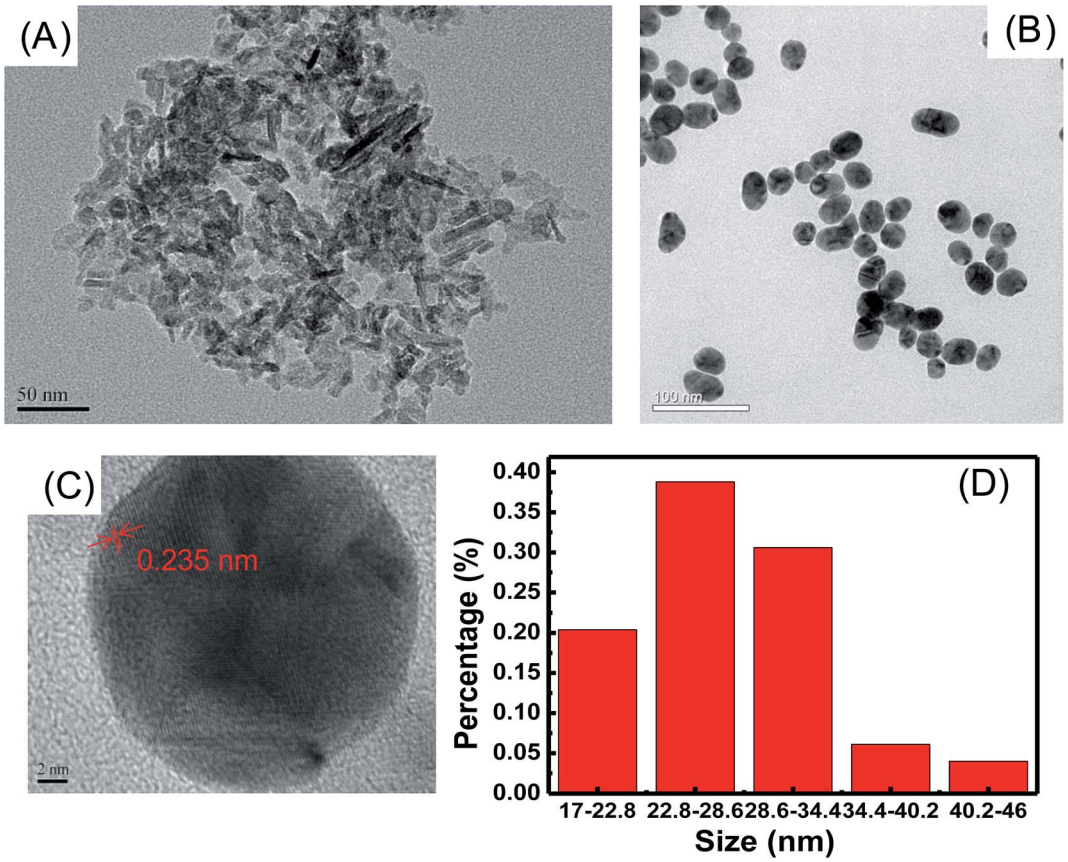

Fig. 1 TEM images of (A) γ-Al_2O_3, (B) Au NPs, (C) HR-TEM image of Au NPs and (D) size distribution of Au NPs.

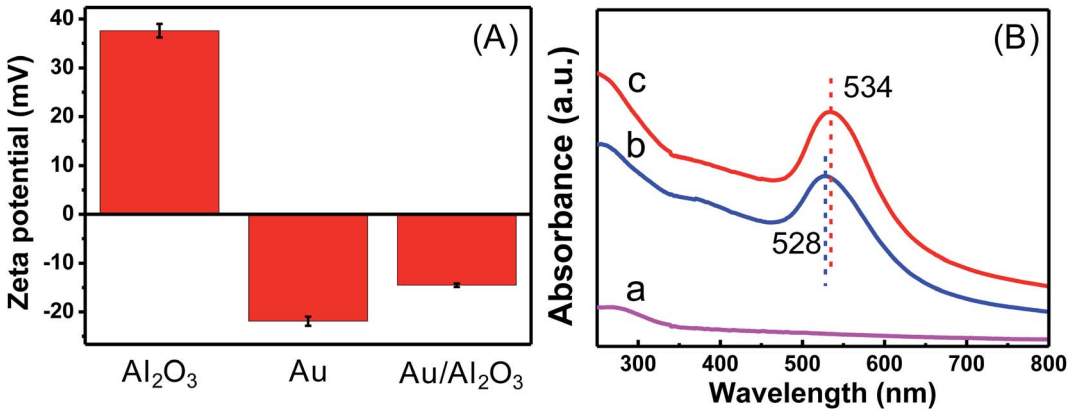

Fig. 2 (A) Zeta potential of γ-Al_2O_3, Au NPs and Au/Al_2O_3 NCs; (B) UV-vis absorption spectra of (a) γ-Al_2O_3, (b) Au NPs and (c) Au/Al_2O_3 NCs.

Aldrich and stored at 4 °C. All the chemicals were of analytical reagent grade and used without further purification. Ultrapure water (18.2 MΩ cm) was produced using a Millipore water purification system and used for all solution preparations. Unless otherwise noted, the synthesis reactions were carried out at room temperature (20 °C–25 °C). Phosphate buffer solution (PBS, 0.1 M, pH = 7) was used and the pH value of PBS buffer was adjusted with dropwise addition of 0.1 M KH_2PO_4 and K_2HPO_4.

2.2. Instruments

Morphologies of Au colloid and Au/Al_2O_3 NCs were observed with a JEOL JEM-2000 FX transmission electron microscope

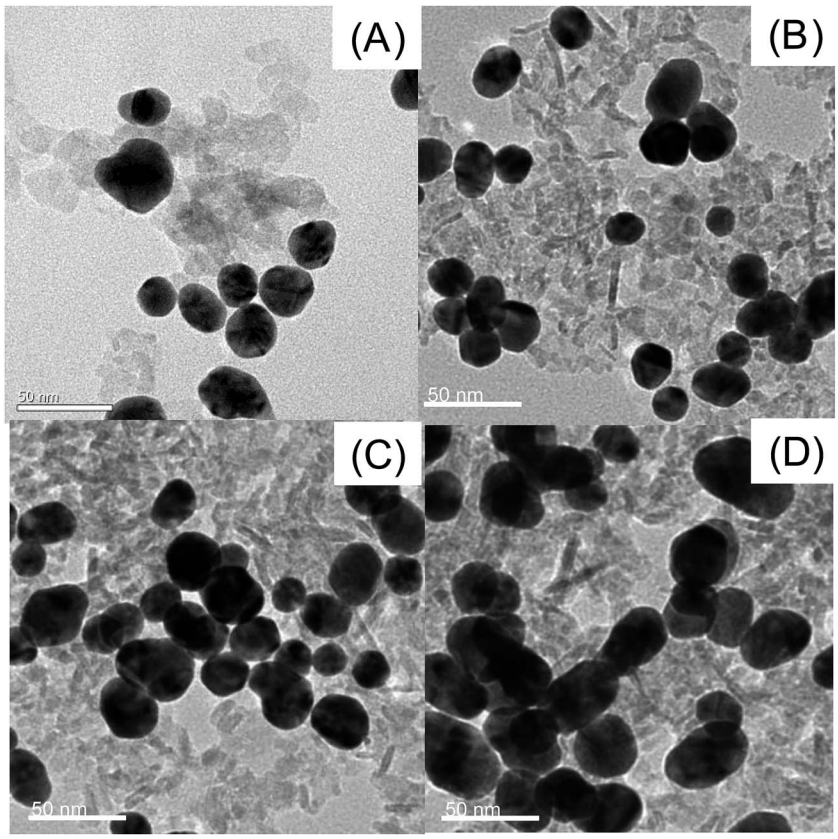

Fig. 3 TEM images of Au/Al_2O_3 NCs synthesized with a fixed amount of Au colloid (10 mL, 0.35 mM) and different volumes of 0.1 M Al_2O_3: (A) 10 μL; (B) 30 μL; (C) 50 μL and (D) 70 μL. Scale bar: 50 nm.

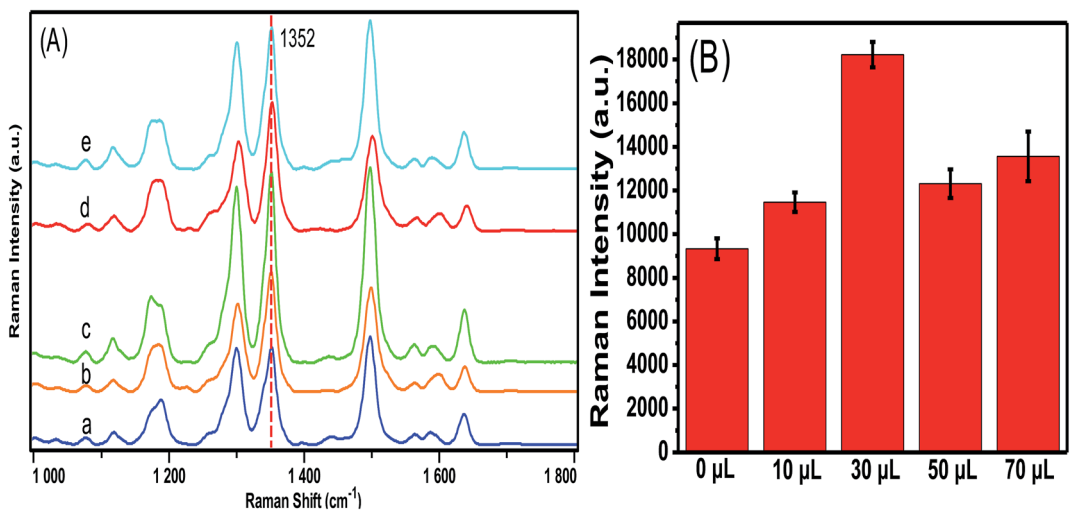

Fig. 4 (A) SERS spectra of 10^{-6} M R6G with Au/Al_2O_3 NCs synthesized with different volumes of 0.1 M Al_2O_3: (a) 0 μL; (b) 10 μL; (c) 30 μL, (d) 50 μL and (e) 70 μL. (B) SERS intensity of the peak at 1352 cm^{-1} for R6G absorbed on Au/Al_2O_3 NCs prepared with different amounts of Al_2O_3.

(TEM) operating at an acceleration voltage of 200 kV. Surface plasmon resonance (SPR) spectra were acquired in a range of 200–800 nm using a UV-7504 UV-visible spectrophotometer (Shanghai XinMao Instrument Co., Ltd.). Zeta potential was monitored with a Zetasizer Nano ZS ZEN3600 (Malvern, UK). Raman measurements were conducted using a Portable Stabilized R. Laser Analyzer (Enwave, USA) with a narrow line width diode laser at 785 nm and an adjustable power with the maximum of 300 mW. X-ray photoelectron spectroscopy (XPS, PHI 5000 VersaProbe) was performed to identify the chemical composition of the surface.

2.3. Preparation of Au/Al_2O_3 NCs as SERS substrate

Colloidal gold was prepared *via* reduction of $HAuCl_4$ by sodium citrate according to the Frens method.[39] Briefly, 0.25 mL of 0.1 M $HAuCl_4$ was added to 100 mL of ultrapure water and heated to boil under vigorous stirring. Then, 1.5 mL of 1% sodium citrate solution was injected into the mixture quickly. The colloid was kept boiling and was stirred for 30 min until it turned wine red.

Afterwards, different volumes (10, 30, 50, 70 μL) of 0.1 M γ-Al_2O_3 suspension liquid were added into 10 mL of 0.35 mM Au colloid and stirred for 1 h to form Au/Al_2O_3 NCs *via* the electrostatic interaction between Au and Al_2O_3. The usage of γ-Al_2O_3 was optimized by the SERS performance of the as-prepared Au/Al_2O_3 NCs with R6G as a model analyte.

2.4. SERS measurements

To get the optimal pH of ATP solution for Raman tests, PBS buffer (PBS, 0.1 M, pH = 7) was adjusted with dropwise addition

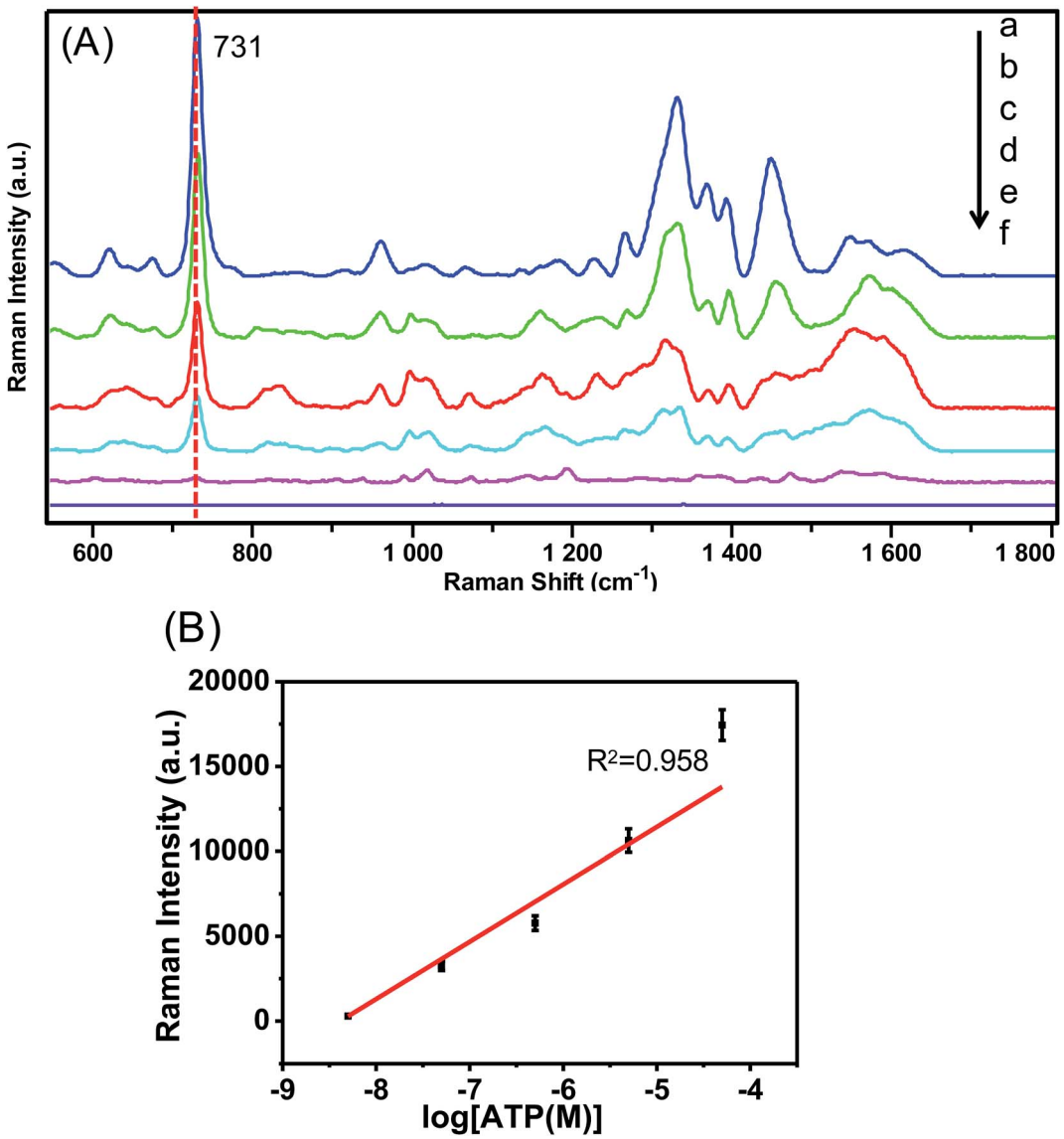

Fig. 5 (A) Concentration-dependent SERS spectra of ATP bound to the optimized Au/Al_2O_3 NCs in a neutral environment (pH = 7). Spectra (a–f) represent the concentrations of ATP being (a) 5×10^{-5}, (b) 5×10^{-6}, (c) 5×10^{-7}, (d) 5×10^{-8}, (e) 5×10^{-9} M and (f) bare substrate as blank control. (B) The linear correlation of Raman intensities at 731 cm^{-1} with the logarithm of ATP concentrations.

of 0.1 M KH_2PO_4 and K_2HPO_4 to pH 3 and pH 10, respectively. After pH optimization, ATP solutions with optimal pH were prepared in a concentration range from 10^{-4} to 10^{-8} M. Then, 5 μL Au/Al_2O_3 NCs and 5 μL ATP solution were mixed together, dropped onto an aluminium foil and dried in the ambient environment for the subsequent Raman test. All the spectra were recorded with the acquisition time of 1 s and accumulation times of 3 s. Unless otherwise mentioned, the accumulation time and the laser power were the same for all Raman measurements.

3 Results and discussion

3.1. Characterization

The morphologies of γ-Al_2O_3 and Au NPs were examined by TEM. The crystallite shape of 20 nm γ-Al_2O_3 is acicular, as shown in Fig. 1A. Fig. 1B shows that Au NPs are uniform and well dispersed on a large scale. Fig. 1C is the HR-TEM image of Au NPs, which shows the crystallinity of the Au NPs. Apparent lattice fringes can be seen and the lattice spacing of two adjacent planes is 0.235 nm, corresponding to the Au (111) plane.[40] The size distribution of Au NPs is displayed in Fig. 1D and the average size is 28 ± 6 nm.

Zeta potential was monitored to observe changes in the surface characteristics during the formation of Au/Al_2O_3 NCs. Au NPs prepared by Frens' method were stabilized by citrate, thus making the surface negatively charged with a measured zeta potential value around −22 mV. The iso-electric point (IEP) of 20 nm γ-Al_2O_3 was around 9,[31] and the surface was positively charged at a pH lower than pH_{IEP}. The zeta potential value of γ-Al_2O_3 dispersed in distilled water was tested and was found to be about 38 mV, which proved that the surface carried the positive charge. Therefore, Au NPs and γ-Al_2O_3 bound together due to electrostatic interaction, and the formation of Au/Al_2O_3 NCs led to a final zeta potential of about −15 mV (see Fig. 2A). UV-visible absorption spectra are revealed in Fig. 2B. γ-Al_2O_3 displays a featureless band as can be seen from curve a. Curve b presents a characteristic SPR band of the prepared Au NPs at 528 nm. After the formation of Au/Al_2O_3 NCs, the SPR band red-shifts to 534 nm, which can be ascribed to the formation of a bigger agglomerate of Au NPs.[41] Au/Al_2O_3 NCs prepared with 30 μL of 0.1 M Al_2O_3 and 10 mL of 0.35 mM Au colloid were used for both zeta potential measurement and the UV-visible absorption test.

3.2. Optimization of SERS performance

Fig. 3 shows TEM images of Au/Al_2O_3 NCs synthesized with different dosage ratios of Au to Al_2O_3. As can be seen, Au NPs are deposited onto the surface of Al_2O_3 and tend to form large agglomerations with the increase in volume of 0.1 M Al_2O_3 from 10 to 70 μL. SERS performance of these four substrates was further analyzed with R6G as the Raman probe and the results are revealed in Fig. 4. It is clear that the highest SERS signal is observed with the addition of 30 μL of 0.1 M Al_2O_3, which can be ascribed to the partial aggregation of Au NPs, but not severe aggregation as observed for the 50 and 70 μL volumes of Al_2O_3. Therefore, Au/Al_2O_3 NCs prepared with 30 μL of 0.1 M Al_2O_3 is chosen as the optimized SERS substrate and used for the following SERS determination of ATP.

3.3. Raman detection of ATP

Before the SERS test of ATP, the effect of pH of the ATP solution on the SERS signal was studied, and the results are given in

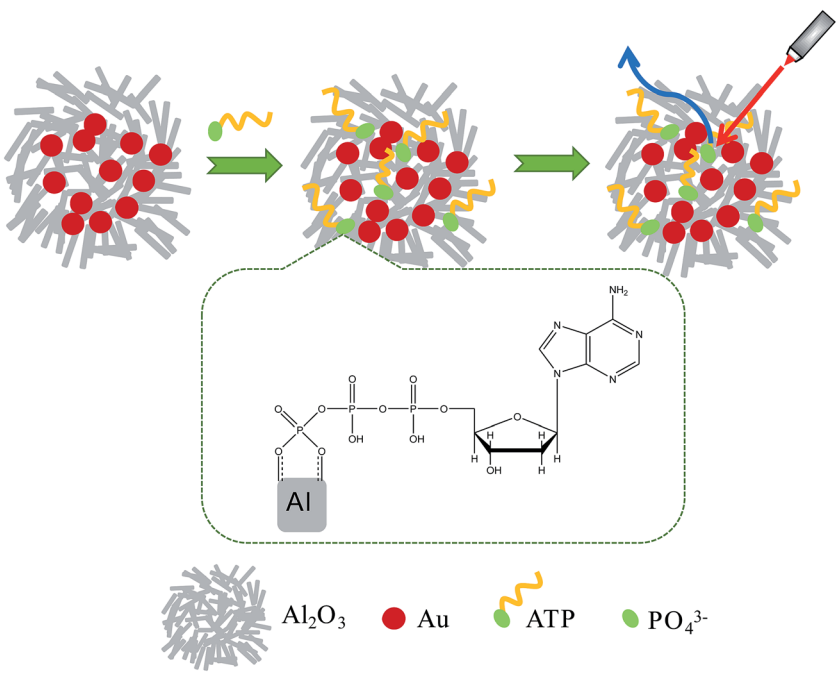

Scheme 1 Schematic of the procedure to detect ATP with Au/Al_2O_3 NCs.

Fig. S1 (ESI†). Raman peaks show a negative shift at pH 7 compared to that at pH 3 due to deprotonation.[42] However, there is no significant shift when pH varies from 7 to 10. Raman intensity of ATP reaches the highest signal at pH 7, and hence SERS determination of ATP is conducted in a neutral environment. Fig. 5A shows the concentration-dependent SERS spectra of ATP at various concentrations from 5×10^{-5} to 5×10^{-9} M with the optimized Au/Al_2O_3 NCs as SERS substrate. The intensities of characteristic peaks increase with an increase in the ATP concentration. The main peaks of ATP molecules are assigned as follows: 680 cm^{-1} (out-of plane wagging of NH_2), 731 cm^{-1} (ring-breathing of adenine ring), 1332 cm^{-1} (C5–N7 stretching), 1450 cm^{-1} (C=N stretching).[35] The lowest detectable concentration is determined as 5×10^{-9} M. Fig. 5B depicts the relationship between SERS intensity of the peak at 713 cm^{-1} and the logarithm of ATP concentration, which demonstrates a good linear relationship ($R^2 = 0.958$) from 5×10^{-5} to 5×10^{-9} M.

In this study, the lowest detectable concentration is lower than that of previously reported methods by 1 order of magnitude.[38] The possible reasons could be inferred as illustrated in Scheme 1 that γ-Al_2O_3 provides a platform to adsorb more ATP molecules onto the SERS substrate area due to aluminum phosphate chelation.[31] The chelation contribution is further proven by careful comparison of XPS patterns of P 2p of ATP bound on Al_2O_3 and pure ATP (see Fig. S2 in ESI†). After ATP binding with Al_2O_3, a positive shift of P 2p binding energy indicates the interaction of the phosphate group with Al_2O_3. Au/Al_2O_3 NCs have also demonstrated a better SERS intensity in detecting ATP than adenosine at the same concentration (see Fig. S3 in ESI†). This chemical control selectivity provided by the supporting material of Al_2O_3 not only helps to further lower the detection limit of ATP but also has the possibility to distinguish ATP and adenosine if multiple elutions are applied in a flow injection combined with SERS detection system. Finally, the partial aggregation of Au NPs on the Al_2O_3 surface may also be responsible for the enhancement of the SERS signal.[29]

4 Conclusions

In summary, a facile protocol was proposed for ATP detection with Au/Al_2O_3 NCs as SERS substrates. Au/Al_2O_3 NCs were prepared *via* the electrostatic interaction between γ-Al_2O_3 and Au NPs and demonstrated good sensitivity with a lowest detectable concentration of 5×10^{-9} M and a good linear relationship from 5×10^{-5} to 5×10^{-9} M. With alumina as the supporting material, the SERS substrate acquired both stability and sensitivity. The low detection limit can be attributed to the partial aggregation of Au NPs onto the γ-Al_2O_3 surface and aluminum phosphate chelation between γ-Al_2O_3 and the phosphate group of ATP. Considering their easy preparation, good sensitivity and short analysis time, Au/Al_2O_3 NCs have potential as a promising SERS substrate for ATP detection.

Acknowledgements

This work is supported by the National Natural Science Foundation of China (No. 21475088) and PCSIRT (IRT-16R49).

References

1 M. Fleischmann, P. J. Hendra and A. J. McQuillan, *Chem. Phys. Lett.*, 1974, **26**, 163–166.
2 M. G. Albrecht and J. A. Creighton, *J. Am. Chem. Soc.*, 1977, **99**, 5215–5217.
3 D. L. Jeanmaire and R. P. Van Duyne, *J. Electroanal. Chem.*, 1977, **84**, 1–20.
4 S. M. Nie and S. R. Emory, *Science*, 1997, **275**, 1102–1106.
5 K. Kneipp, Y. Wang, H. Kneipp, L. T. Perelman, I. Itzkan, R. R. Dasari and M. S. Feld, *Phys. Rev. Lett.*, 1997, **78**, 1667–1670.
6 D. Radziuk and H. Moehwald, *Phys. Chem. Chem. Phys.*, 2015, **17**, 21072–21093.
7 A. H. Nguyen, Y. Shin and S. J. Sim, *Biosens. Bioelectron.*, 2016, **85**, 522–528.
8 H. Jang, E. Y. Hwang, Y. Kim, J. Choo, J. Jeong and D. W. Lim, *J. Biomed. Nanotechnol.*, 2016, **12**, 1938–1951.
9 X. Hu, P. Zheng, G. Meng, Q. Huang, C. Zhu, F. Han, Z. Huang, Z. Li, Z. Wang and N. Wu, *Nanotechnology*, 2016, **27**, 384001.
10 M. Jahn, S. Patze, T. Bocklitz, K. Weber, D. Cialla-May and J. Popp, *Anal. Chim. Acta*, 2015, **860**, 43–50.
11 T. Yang, X. Guo, Y. Wu, H. Wang, S. Fu, Y. Wen and H. Yang, *ACS Appl. Mater. Interfaces*, 2014, **6**, 20985–20993.
12 B. Tang, J. Wang, J. A. Hutchison, L. Ma, N. Zhang, H. Guo, Z. Hu, M. Li and Y. Zhao, *ACS Nano*, 2016, **10**, 871–879.
13 W. A. El-Saida, D. M. Fouada and S. A. El-Safty, *Sens. Actuators, B*, 2016, **228**, 401–409.
14 Z. Han, H. Liu, J. Meng, L. Yang and J. Liu, *Anal. Chem.*, 2015, **87**, 9500–9506.
15 B. Sägmüller, B. Schwarze, G. Brehm and S. Schneider, *Analyst*, 2001, **126**, 2066–2071.
16 D. Han, S. Y. Lim, B. J. Kim, L. Piao and T. D. Chung, *Chem. Commun.*, 2010, **46**, 5587–5589.
17 S. S. R. Dasary, A. K. Singh, D. Senapati, H. Yu and P. C. Ray, *J. Am. Chem. Soc.*, 2009, **131**, 13806–13812.
18 S. J. Lee and M. Moskovits, *Nano Lett.*, 2011, **11**, 145–150.
19 A. Barhoumi and N. J. Halas, *J. Am. Chem. Soc.*, 2010, **132**, 12792–12793.
20 R. Li, S. Li, M. Dong, L. Zhang, Y. Qiao, Y. Jiang, W. Qi and H. Wang, *Chem. Commun.*, 2015, **51**, 16131–16134.
21 J. Jia, K. Haraki, J. N. Kondo, K. Domen and K. Tamaru, *J. Phys. Chem. B*, 2000, **104**, 11153–11156.
22 J. Radnik, L. Wilde, M. Schneider, M. M. Pohl and D. Herein, *J. Phys. Chem. B*, 2006, **110**, 23688–23693.
23 M. Pisarek, R. Nowakowski, A. Kudelski, M. Holdynski, A. Roguska, M. Janik-Czachor, E. Kurowska-Tabor and G. D. Sulka, *Appl. Surf. Sci.*, 2015, **357**, 1736–1742.
24 P. Nielsen, S. Hassing, O. Albrektsen, S. Foghmoes and P. Morgen, *J. Phys. Chem. C*, 2009, **113**, 14165–14171.
25 K. Malek, A. Brzózka, A. Rygula and G. D. Sulka, *J. Raman Spectrosc.*, 2014, **45**, 281–291.
26 K. D. Jernshøj, S. Hassing, R. S. Hansen and P. Krohne-Nielsen, *J. Chem. Phys.*, 2011, **135**, 124514.

27 C. C. Chang, C. C. Yu, Y. C. Liu and K. H. Yang, *J. Electroanal. Chem.*, 2013, **696**, 38–44.
28 F. D. Mai, K. H. Yang, Y. C. Liu and T. C. Hsu, *Analyst*, 2012, **137**, 5906–5912.
29 F. D. Mai, C. C. Yu, K. H. Yang and M. Y. Juang, *J. Phys. Chem. C*, 2011, **115**, 13660–13666.
30 X. Zhang, J. Zhao, A. V. Whitney, J. W. Elam and R. P. Van Duyne, *J. Am. Chem. Soc.*, 2006, **128**, 10304–10309.
31 Y. Yan, L. K. Koopal, W. Li, A. Zheng, J. Yang, F. Liu and X. Feng, *J. Colloid Interface Sci.*, 2015, **451**, 85–92.
32 F. Y. Kuo, B. Y. Chang, C. Y. Wu, K. K. T. Mong and Y. C. Chen, *Anal. Chem.*, 2015, **87**, 10513–10520.
33 J. Ross, *J. Phys. Chem. B*, 2006, **110**, 6987–6990.
34 T. Tenório, A. M. Silva, J. M. Ramos, C. D. Buarque and J. Felcman, *Spectrochim. Acta, Part A*, 2013, **105**, 88–101.
35 A. Lanir and N. T. Yu, *J. Biol. Chem.*, 1979, **254**, 5382–5887.
36 T. T. Chen, C. S. Kuo, Y. C. Chou and N. T. Liang, *Langmuir*, 1989, **5**, 887–891.
37 M. Li, J. Zhang, S. Suri, L. J. Sooter, D. Ma and N. Wu, *Anal. Chem.*, 2012, **84**, 2837–2842.
38 H. Fang, H. J. Yin, M. Y. Lv, H. J. Xu, Y. M. Zhao, X. Zhang, Z. L. Wu, L. Liu and T. W. Tan, *Biosens. Bioelectron.*, 2015, **69**, 71–76.
39 G. Frens, *Nature*, 1973, **241**, 20–22.
40 T. Yang, X. Guo, H. Wang, S. Fu, Y. Wen and H. Yang, *Biosens. Bioelectron.*, 2015, **68**, 350–357.
41 Y. Lin, C. Chen, C. Wang, F. Pu, J. Ren and X. Qu, *Chem. Commun.*, 2011, **47**, 1181–1183.
42 R. A. Alberty, *J. Biol. Chem.*, 1968, **243**, 1337–1343.